Journal of Aerospace Technology and Management
ISSN: 1984-9648
secretary@jatm.com.br
Instituto de Aeronáutica e Espaço
Brasil

Forgas Júnior, Arnaldo; Otubo, Jorge; Magnabosco, Rodrigo
Ferrite Quantification Methodologies for Duplex Stainless Steel
Journal of Aerospace Technology and Management, vol. 8, núm. 3, julio-septiembre, 2016, pp. 357-362
Instituto de Aeronáutica e Espaço
São Paulo, Brasil

Available in: http://www.redalyc.org/articulo.oa?id=309446752011

How to cite
Complete issue
More information about this article
Journal's homepage in redalyc.org

Scientific Information System
Network of Scientific Journals from Latin America, the Caribbean, Spain and Portugal
Non-profit academic project, developed under the open access initiative

doi: 10.5028/jatm.v8i3.653

Ferrite Quantification Methodologies for Duplex Stainless Steel

Arnaldo Forgas Júnior[1], Jorge Otubo[1], Rodrigo Magnabosco[2]

ABSTRACT: In order to quantify ferrite content, three techniques, XRD, ferritoscope and optical metallography, were applied to a duplex stainless steel UNS S31803 solution-treated for 30 min at 1,000, 1,100 and 1,200 °C, and then compared to equilibrium of phases predicted by ThermoCalc® simulation. As expected, the microstructure is composed only by austenite and ferrite phases, and ferrite content increases as the solution treatment temperature increases. The microstructure presents preferred grains orientation along the rolling directions even for a sample solution treated for 30 min at 1,200 °C. For all solution treatment temperatures, the ferrite volume fractions obtained by XRD measurements were higher than those achieved by the other two techniques and ThermoCalc® simulation, probably due to texturing effect of previous rolling process. Values obtained by quantitative metallography look more assertive as it is a direct measurement method but the ferritoscope technique should be considered mainly for *in loco* measurement.

KEYWORDS: Duplex stainless steels, Ferrite quantification, Ferritoscope, Quantitative metallography, X-ray diffraction, ThermoCalc®.

INTRODUCTION

Duplex stainless steels (DSS) are characterized ideally by equal amounts of ferrite and austenite, which provides increased mechanical resistance (680 to 880 MPa ultimate tensile strength) due to the fine grain size, typical of these steels (Sedriks 1996; Souza *et al.* 2005). They present higher corrosion resistance when compared to ferritic stainless steels, promoted by high content of chromium, nitrogen and molybdenum, and, due to the presence of austenite, the DSS present good ductility and toughness (250 J impact toughness) (Young *et al.* 2007).

This behavior (corrosion resistance, strength) is promoted by the presence of approximately 50% volume fraction of ferrite (Kashiwar *et al.* 2012), and therefore the control of the ferrite content in DSS is necessary to ensure the desired properties.

DSS form a specific group of materials that are used in a variety of industrial applications. The main factor that makes these materials useful for the production of components for the chemical, food and aerospace industries, which requires long-life components, are precisely their high corrosion resistance and mechanical strength (Oliveira *et al.* 2014).

Nowadays, the use of DSS has grown considerably in several applications, such as, for pressure vessels, heat exchangers, pipelines, evaporators, storage towers and pipelines in oil and gas industries for transportation of dry and/or wet carbon dioxide (Kashiwar *et al.* 2012) and rod technologies developed in the aerospace industry (Badoo 2008). DSS are also used on a large scale in the construction of off-shore platforms, in seawater injection systems and systems applied for removal of CO_2 and H_2S (Souza *et al.* 2005).

1.Departamento de Ciência e Tecnologia Aeroespacial – Instituto Tecnológico de Aeronáutica – Divisão de Engenharia Aeronáutica e Mecânica – São José dos Campos/SP – Brazil. **2.**Fundação Educacional Inaciana – São Bernardo do Campo/SP – Brazil.

Author for correspondence: Arnaldo Forgas Júnior | Departamento de Ciência e Tecnologia Aeroespacial – Instituto Tecnológico de Aeronáutica – Divisão de Engenharia Aeronáutica e Mecânica | Praça Marechal Eduardo Gomes, 50 – Vila das Acácias | CEP: 12.228-900 – São José dos Campos/SP – Brazil | Email: forgas.jr@gmail.com

Received: 03/24/2016 | **Accepted:** 05/05/2016

The increase of the demand for DSS in industrial applications made mandatory the control of the manufacturing processes and the necessity to know accurately the quantities of the phases before the final use. Unfortunately, the phase quantification can be influenced by the existing measurement techniques. Previous studies (Magnabosco and Spomberg 2011; Tavares *et al.* 2012) showed quantification of the ferrite volume fraction of DSS using two different techniques: quantitative metallography after Beraha etching and magnetic measurements with a ferritoscope. The results showed considerable discrepancies between the values obtained by these techniques (Magnabosco and Spomberg 2011).

Another technique to evaluate the volume fraction of the phases is by analysis of the peak intensity of X-ray diffraction (XRD) patterns. For a randomly oriented DSS sample, quantitative measurements of the relative ferrite and austenite content can be obtained from XRD patterns taking into account the total integrated intensity of all diffraction peaks for each phase, which is proportional to the volume fraction of that phase. If the crystalline phase or grains of each phase are randomly oriented, the integrated intensity from any single diffraction peak related to a (*hkl*) crystalline plane is also proportional to the volume fraction of that phase (ASTM E 975-13; Cullity and Stock 2001).

The main objective of this research is to compare different methodologies of ferrite phase quantification: quantitative optical metallography, magnetic measurement by ferritoscope and analysis of the peak intensities of the phases by X-ray diffraction, comparing them to the equilibrium of phases predicted by ThermoCalc® simulation.

EXPERIMENTAL PROCEDURES

The studied material is a hot rolled DSS (UNS S31803) plate 300 mm long × 200 mm wide × 3 mm thick with the chemical composition shown in Table 1.

Samples from the original plate were solution-treated under nitrogen atmosphere at three different temperatures, 1,000, 1,100 and 1,200 °C, for 30 min, and then cooled in water. For each temperature, the solution-treated strips samples were cut into specimens of 10 × 10 mm and subsequently embedded in thermosetting resin. The samples were analyzed considering the plan surface of the plate viewing from the rolling direction. Further, the specimens were ground to 500-mesh emery paper and then polished down to 1 μm size diamond paste lubricated with ethanol in a semi-automatic polishing equipment.

After polishing, the microstructures of the specimens were revealed with modified Beraha etchant (20 mL of hydrochloric acid + 80 mL of distilled and deionized water), and to this stock solution 1 g of potassium metabisulphite + 2 g of ammonium bifluoride were added just before etching. The etching time was approximately 30 s, and the etching was interrupted by immersion in water. The surfaces after etching were dried by ethanol evaporation, aided by a cold air jet, enabling the micrograph recording of the samples.

The volume fraction of ferrite was quantified by three different techniques:

- Magnetic measurement by ferritoscope: after polishing of the specimens, ten measurements of the volume fraction of ferrite of each sample were taken with a FISCHER MP30 ferritoscope; the equipment was calibrated with appropriate standards, with detection limit of 0.1% ferrite. The ferritoscope is a method that measures the fraction of the ferromagnetic phase. The measurement method is based on magnetic induction in which a magnetic field is generated by a coil that interacts with the magnetic phase of the sample. The changes in the magnetic field induce a voltage proportional to the ferromagnetic phase content in a second coil. This voltage is then evaluated.
- Quantitative optical metallography: after polishing and etching, measurements of phase contents were made by the point counting technique prescribed in ASTM Standard E562-02, using an image analysis routine with Leica QMetals software, connected to a Leica DMLM microscope. Ten fields per sample were analyzed at 500X magnification.
- X-ray diffraction: to confirm the existence of ferrite and austenite, X-ray diffraction patterns were obtained using a Shimadzu XRD-7000 diffractometer under Cu-Kα radiation; diffraction scans were performed at $30° < 2\theta < 120°$ at a rate of 1°/min and sampling every 0.04°; Cu source was excited at acceleration voltage of 30 kV and current of 30 mA.

Table 1. Chemical composition (mass percentage) of DSS.

Cr	Ni	Mo	Mn	N	C	Si	P	S	Fe
22.07	5.68	3.20	1.38	0.17	0.017	0.34	0.02	0.001	Balance

The method used to determine phase content from XRD tests was described in the study of Moser *et al.* (2014). The quantitative estimation is based on the use of internal ratios. Assuming that the grains are randomly oriented, the integrated intensity of a given phase *i* is proportional to the volume fraction of that phase, *Vi*, as shown in Eq. 1:

$$V_i = \frac{\frac{1}{n}\Sigma_1^n \frac{I_i^j}{R_i^j}}{\frac{1}{n}\Sigma_1^n \frac{I_\gamma^j}{R_\gamma^j} + \frac{1}{n}\Sigma_1^n \frac{I_\alpha^j}{R_\alpha^j}} \quad (1)$$

where: n is the number of peaks examined for each phase (being i the phases γ or α); j = 1, 2, 3, …, n; R is the material scattering factor and is described in Eq. 2:

$$R_{hkl} = \left(\frac{1}{V^2}\right)\left[|F|p\left(\frac{1+\cos^2 2\theta}{\sin^2\theta\cos\theta}\right)\right]e^{-2M} \quad (2)$$

where: V is the volume fraction of the unit cell; F is the structure factor; *hkl* are the Miller indexes of the reflection plane; p is the multiplying factor associated to the specific *hkl* plane; θ is the diffraction angle; and e^{-2M} is Debye-Waller Factor (DWF).

Table 2 shows the values of those variables for specific planes of typical austenite and ferrite phases. The volume fraction of the unit cell V is obtained through the lattice parameter a of ferrite and austenite, determined from XRD patterns after the application of the Nelson-Riley extrapolation method for accurate unit-cell dimensions of crystals (Nelson and Riley 1945).

Equilibrium in the solution-treatment temperatures was predicted by ThermoCalc® software using TCFe7 database, inputting in the software:

- Chemical composition according to Table 1.
- Temperature range (1,000 to 1,200 °C).

Table 2. Values for the determination of the material scattering factor for specific planes of ferrite and austenite in stainless steels (ASTM E 975-13; Cullity and Stock 2001).

Austenite (FCC)				Ferrite (BCC)			
hkl	*F*	*p*	*DWF*	*hkl*	*F*	*p*	*DWF*
(111)	17.454	8	0.960	(110)	17.285	12	0.958
(200)	16.460	6	0.947	(200)	14.695	6	0.918
(220)	13.703	12	0.897	(211)	12.994	24	0.880
(311)	12.345	24	0.861	(220)	11.752	12	0.843

FCC: Face centred cubic; BCC: Body centred cubic.

So, it is possible to analyze the measured ferrite contents by the three described methods and the expected equilibrium ferrite fraction from ThermoCalc® simulation.

RESULTS AND DISCUTION

Figures 1, 2 and 3 show, respectively, the micrographs of specimens' solution treated at 1,000, 1,100 and 1,200 °C etched with modified Beraha reagent. It is verified the presence of only two phases: ferrite (dark gray) and austenite (light gray), as expected (Nilsson 1992; Nilsson and Chai 2012).

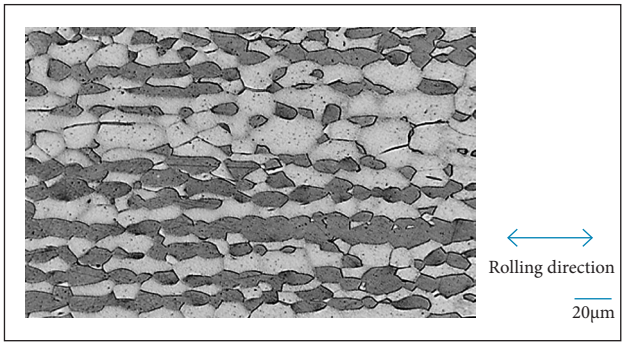

Figure 1. Micrograph of the sample heat-treated at 1,000 °C.

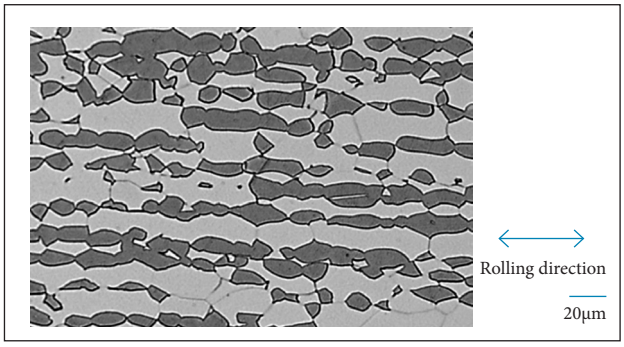

Figure 2. Micrograph of the sample heat-treated at 1,100 °C.

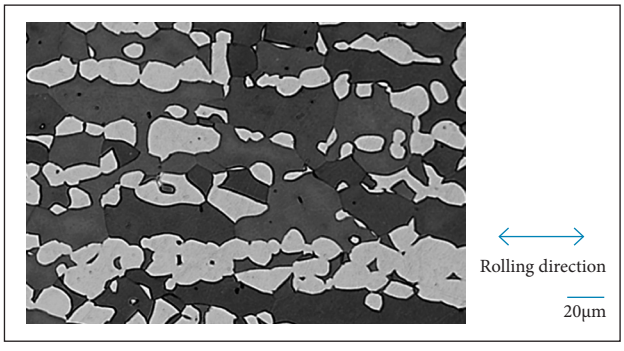

Figure 3. Micrograph of the sample heat-treated at 1,200 °C.

Micrographs showed that ferrite and austenite grains distribution present a preferred orientation in the rolling direction as indicated by double arrows. Those preferred grains orientation decreased but it was not completely eliminated as the solution treatment temperatures increase, and the random structure needed for quantitative optical microscopy and XRD determination of ferrite phase previously discussed is impaired. As expected, the increase in solution treatment temperature leads to larger grain sizes.

Figures 4, 5 and 6 present XRD patterns for samples solution treated at 1,000, 1,100 and 1,200 °C, respectively, showing that only ferrite and austenite phases are identified

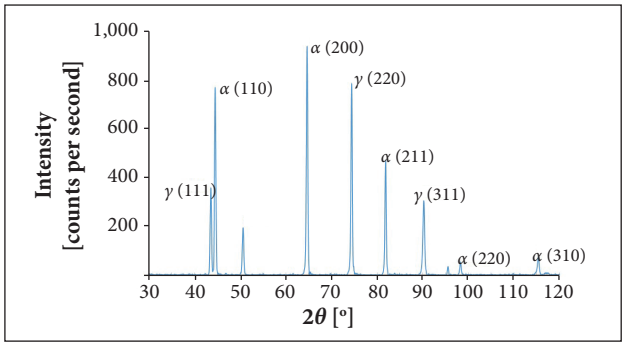

Figure 4. X-Ray diffraction for sample solution treated at 1,000 °C.

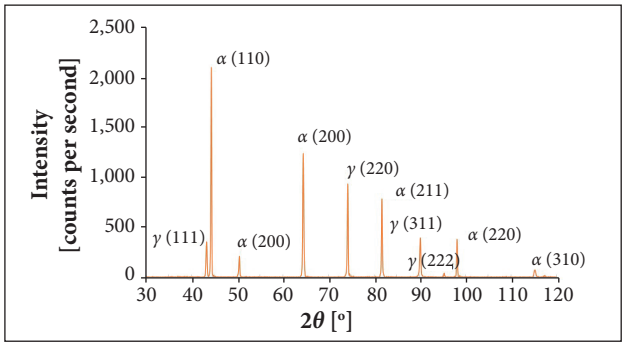

Figure 5. X-ray diffraction for sample solution treated at 1,100 °C.

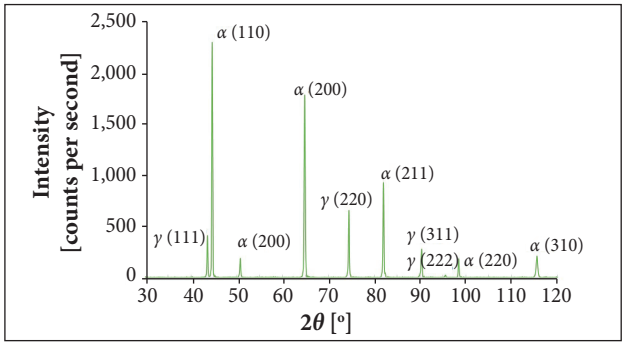

Figure 6. X-ray diffraction for sample solution treated at 1,200 °C.

in the microstructures, confirming the observations of optical micrographs (Figs. 1 to 3). The unit cell parameters (*a*) for ferrite and austenite (calculated from XRD results) were, respectively, 0.2880 and 0.3601 nm in all solution-treatment temperatures, and the respective unit cell (*V*) volumes were 0.023879 and 0.046711 nm^3.

Duplex stainless steel solidifies from liquid phase through ferritic field, and between 1,200 and 1,000 °C, approximately, ferrite plus austenite area is achieved. In this field, it forms duplex structure. Since the fractions of ferrite and austenite may be calculated, these relative fractions can be controlled by selecting the appropriate heating temperature (Nilsson 1992). Figure 7 illustrates this variation as a function of solution-treated temperature obtained by ThermoCalc® software with TCFE7 database. It is noted that the phases present in this temperature range are only ferrite and austenite, and, as expected, with increasing solution-treated temperature higher is the volume fraction of ferrite.

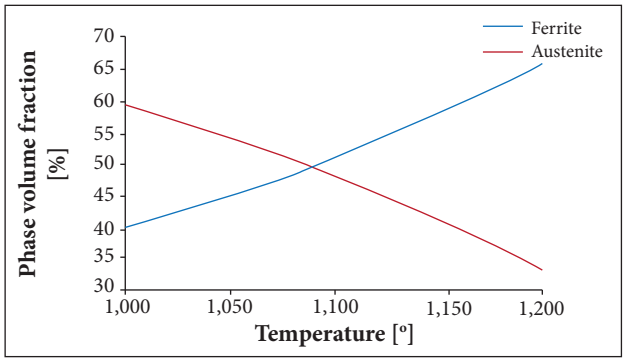

Figure 7. Results from ThermoCalc® software simulation showing only two equilibrium phases, from 1,000 to 1,200 °C temperature range.

Table 3 presents the ferrite volume fraction of the solution-treated samples at 1,000, 1,100 and 1,200 °C for all techniques: XRD, ferritoscope, quantitative optical metallography and also ThermoCalc® prediction. It can be noted that increasing the solution-treatment temperature the ferrite content increases as well, considering all applied techniques.

Figure 8 shows a comparison between the values of ferrite volume fraction obtained by these methodologies, XRD, ferritoscope, and quantitative optical microscopy, all of them compared to ThermoCalc® prediction.

This figure could be separated into two regions: region 1 corresponding to higher ferrite volume fraction varying from

Table 3. Ferrite content by measurement techniques.

Temperature (°C)	Ferrite content (%)			
	XRD	Ferritoscope	Quantitative optical microscopy	ThermoCalc®
1,000	58.4	39.8 ± 0.5	41.5 ± 0.9	40.4
1,100	68.5	46.2 ± 0.5	48.1 ± 0.8	51.3
1,200	87.2	57.0 ± 0.7	58.5 ± 1.5	66.4

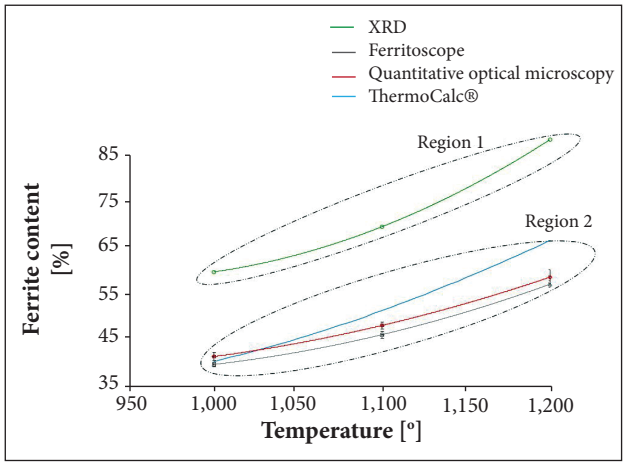

Figure 8. Ferrite content obtained by the four measuring techniques.

56 to 88%, obtained by XRD measurements, and region 2 with lower ferrite content varying from 40 to 66%, obtained by the other methods (quantitative optical metallography, ferritoscope and ThermoCalc® prediction), both taking into account the solution-treated temperatures.

The high values of ferrite content, region 1, presented by XRD measurements, could be attributed to the preferred grains orientations that persist even for the solution-treated sample at 1,200 °C conditioned to the previous hot rolled 3 mm thick plate. Nevertheless, all techniques show the same trend of increasing ferrite volume fraction with increasing solution-treated temperature, as provided in ThermoCalc®.

In region 2, it is verified that solution-treated samples at 1,000 °C produced similar results comparing the two techniques, quantitative microscopy and ferritoscope, to the equilibrium prediction of ThermoCalc® simulation. However, at 1,100 and 1,200 °C, the result obtained by ThermoCalc® simulation was higher than that obtained by quantitative microscopy and ferritoscope, increasing proportionally as the solution treatment temperature increases. This difference could be attributed to the fact that ThermoCalc® simulation does not take into account texture and especially grain size, which can affect the kinetics of phase formation. Quantitative microscopy and ferritoscope showed equivalent results as far as the differences are within the experimental errors. It can be concluded that values obtained by quantitative optical microscopy could be more assertive as far as it is a direct measurement method, but ferritoscope technique could be a fast alternative tool for ferrite quantification *in loco*. All three techniques, although giving different results, showed clearly the tendency of the increase the volume fraction of ferrite as the solution treatment temperature increases, in accordance with the equilibrium prediction.

CONCLUSIONS

Different techniques were used to quantify the volume fraction of ferrite in a duplex stainless steel and were compared with ThermoCalc® simulations. All of them showed clearly the increase in ferrite content as the solution treatment temperature increases.

The plot of ferrite content as a function of solution treatment temperature showed two distinct regions, one related to XRD technique, presenting higher values of volume fraction, and another region with lower values obtained by optical metallography, ferritoscope techniques and ThermoCalc® simulations.

The higher values of ferrite content presented by XRD technique could be attributed possibly to the influence of the texture imposed by hot rolling, as the preferred grains orientation along the rolling direction is not eliminated even in a solution treatment at 1,200 °C.

Quantitative metallography seems to be the most assertive technique to measure volume fraction of the phases in DSS, but ferritoscope technique should be considered for practical applications such as *in loco* measurement.

REFERENCES

Badoo NR (2008) Stainless steel in construction: a review of research, applications, challenges and opportunities. Journal of Constructional Steel Research 64(11):1199-1206. doi: 10.1016/j.jcsr.2008.07.011

Cullity BD, Stock SR (2001) Elements of X-ray diffraction. 3rd ed. New Jersey: Prentice-Hall.

Kashiwar A, Vennela N, Kamath SL, Kathirkar RK (2012) Effect of solution annealing temperature on precipitation on 2205 duplex stainless steel. Mater Char 74:55-63. doi: 10.1016/j.matchar.2012.09.008

Magnabosco R, Spomberg S (2011) Comparative study of ferrite quantification methods applied to duplex stainless steel. Proceedings of the 7th European Stainless Steel Conference — Science and Market; Milan, Italy.

Moser NH, Gross TS, Korkolis YP (2014) Martensite formation in conventional and isothermal tension of 304 austenitic stainless steel measured by X-ray diffraction. Metall Mater Trans 45(11):4891-4896. doi: 10.1007/s11661-014-2422-y

Nelson JB, Riley DP (1945) An experimental investigation of extrapolation methods in the derivation of accurate unit-cell dimensions in crystals. Proc Phys Soc 57(3):160-177. doi: 10.1088/0959-5309/57/3/302

Nilsson JO (1992) Super duplex stainless steels. Materials Science and Technology 8(8):685-700. doi: 10.1179/mst.1992.8.8.685

Nilsson JO, Chai G (2012) The physical metallurgy of duplex stainless steel. Sandvik Materials Technology, R&D Centre, S-81181. Sandviken: Sandvik Materials Technology.

Oliveira CA, Diniz AE, Bertazzoli R (2014) Correlating tool wear, surface roughness and corrosion resistance in the turning process of super duplex stainless steel. J Braz Soc Mech Sci Eng 36(4):775-785. doi: 10.1007/s40430-013-0119-6

Sedriks AJ (1996) Corrosion of stainless steel. 2nd ed. New York: John Wiley.

Souza GC, Pardal JM, Tavares SSM, Fonseca MPCF, Martins JLF, Moura EP, Cardote IF (2005) Evaluation of proportion of phases in joints welded from duplex stainless steel pipes by means of non-destructive testing. Weld Int 29(10):762-770. doi: 10.1080/09507116.2014.932985

Tavares SSM, Pardal JM, Abreu HFG, Nunes CS, Silva MR (2012) Tensile properties of duplex UNS s32205 and lean duplex UNS S32304 steels and the influence of short duration 475 °C aging. Materials Research 15(6):859-864. doi: 10.1590/S1516-14392012005000116

Young MC, Tsay LW, Shin CS, Chan SLI (2007) The effect of short time post-weld heat treatment on the fatigue crack growth of 2205 duplex stainless steel welds. Int J Fatig 29(12):2155-2162. doi: 10.1016/j.ijfatigue.2007.01.004